JBC Papers in Press. Published on May 22, 2017 as Manuscript M117.792200
The latest version is at http://www.jbc.org/cgi/doi/10.1074/jbc.M117.792200

Heme-thiolate sulfenylation of human cytochrome P450 4A11 functions as a redox switch for catalytic inhibition*[S]

Matthew E. Albertolle[1], Donghak Kim[1,2], Leslie D. Nagy[1], Chul-Ho Yun[3], Ambra Pozzi[4,5], Üzen Savas[6], Eric F. Johnson[6], and F. Peter Guengerich[1]

[1]Department of Biochemistry, Vanderbilt University School of Medicine, Nashville, Tennessee 37232-0146, [2]Department of Biological Sciences, Konkuk University, Seoul 05025, Republic of Korea, [3]School of Biological Sciences and Technology, Chonnam National University, Gwangju 61186, Republic of Korea, [4]Department of Medicine, Vanderbilt University Medical Center, Nashville, Tennessee 37232-6602, [5]Veterans Affairs Medical Center, Nashville, Tennessee, 37232, and [6]Department of Molecular Medicine, The Scripps Research Institute, La Jolla, California 92037

Running title: *P450 4A11 Sulfenic Acid and Inhibition*

Address correspondence to: Prof. F. Peter Guengerich, Department of Biochemistry, Vanderbilt University School of Medicine, 638B Robinson Research Building, 2200 Pierce Avenue, Nashville, Tennessee 37232-0146, Telephone: (615) 322-2261; FAX: (615) 343-0704; E-mail: f.guengerich@vanderbilt.edu

Keywords: Cytochrome P450, mass spectrometry, proteomics, thiol, oxidative damage

ABSTRACT

Cytochrome P450 (P450, CYP) 4A11 is a human fatty acid ω-hydroxylase that catalyzes the oxidation of arachidonic acid to the eicosanoid 20-hydroxyeicosatetraenoic acid (20-HETE), which plays important roles in regulating blood pressure regulation. Variants of P450 4A11 have been associated with high blood pressure and resistance to anti-hypertensive drugs, and 20-HETE has both pro- and antihypertensive properties relating to increased vasoconstriction and natriuresis, respectively. These physiological activities are likely influenced by the redox environment, but the mechanisms are unclear. Here, we found that reducing agents (e.g., dithiothreitol and *tris*(carboxyethyl)phosphine) strongly enhanced the catalytic activity of P450 4A11, but not of 10 other human P450s tested. Conversely, added H_2O_2 attenuated P450 4A11 catalytic activity. Catalytic roles of five of the potentially eight implicated Cys residues of P450 4A11 were eliminated by site-directed mutagenesis. Using an isotope-coded dimedone/iododimedone labeling strategy and mass spectrometry of peptides, we demonstrated that the heme-thiolate cysteine (Cys-457) is selectively sulfenylated in a H_2O_2 concentration-dependent manner. This sulfenylation could be reversed by reducing agents, including dithiothreitol and dithionite. Of note, we observed heme ligand cysteine sulfenylation of P450 4A11 e*x vivo* in kidneys and livers derived from *CYP4A11* transgenic mice. We also detected sulfenylation of murine P450s 4a12 and 4b1 heme peptides in kidneys. To our knowledge, reversible oxidation of the heme thiolate has not previously been observed in P450s, to our knowledge, and may have relevance for 20-HETE-mediated functions.

Human cytochrome P450 (P450, CYP) enzymes catalyze oxidations of numerous endogenous substrates, including eicosanoids, steroids, and vitamins (1). At least 13 human P450 enzymes (2C8, 2C9, 2J2, 2U1, 4A11, 4F22, 4F12, 4V2, 4F2, 4F3, 4F8, 5A1, and 8A1) utilize fatty acids and/or eicosanoids as substrates (2). P450 4A11 is primarily an ω-hydroxylase, with its main endogenous role apparently being the conversion of arachidonic acid to 20-hydroxyeicosatetraenoic acid (20-HETE) (3). P450 4A11 can also catalyze oxidations of other fatty acid substrates, including lauric acid (4):

$$CH_3(CH_2)_nCO_2H \longrightarrow HOCH_2(CH_2)_nCO_2H$$

P450 4A11 is expressed mainly in the liver, kidney, and vasculature (5,6), and Subfamily

4A P450 enzymes have been associated with vascular dysfunction and hypertension in rodent models and humans (7). The P450 4A11 F434S variant has been associated with increased blood pressure in several populations studied (8-13). 20-HETE plays opposing roles, having both pro- and anti-hypertensive actions by promoting vasoconstriction or natriuresis, respectively (14). 20-HETE has been reported to induce transcription of NADPH oxidase, activating this enzyme complex through protein kinase C (15-18), and has also been reported to increase mitochondrial reactive oxygen species (ROS) production (19). Studies with P450 4A11 transgenic mice have identified P450 4A11 regulation via fasting and growth hormone (20) and that 20-HETE and P450 4A11 activity may uncouple the renal renin angiotensin system (21).

ROS, specifically H_2O_2, have recently become regarded as important secondary signaling molecules (22). H_2O_2 modifies epidermal growth factor receptor signaling (23) and regulates glycolysis through glyceraldehyde-3-phosphate dehydrogenase (24). Common targets of H_2O_2 are protein thiols, oxidizing them to more reactive species, mainly sulfenic acids (-SOH). This transient posttranslational modification aids in the formation of inter- or intra-molecular disulfide bonds, alters cellular signaling, and regulates enzymatic activity (25,26).

In this study, we noted the stimulation of P450 4A11 activity by thiols and other reducing agents and further examined the ability of P450 4A11 to respond to perturbations in the redox environment *in vitro*. Ten other recombinant human P450s were tested for sensitivity to reductants and no large changes in activity were noted. Five of the eight possible cysteine (to serine) mutants of P450 4A11 were expressed and were found to be catalytically active, reducing the possibilities for the sensitive thiol. We observed that P450 4A11 is sensitive to oxidation and, interestingly, sulfenic acid formation was able to disrupt binding of Cys-457 to the heme iron and inactivate the enzyme, in a very reversible process. We also detected sulfenylation of P450 4A11 and murine Subfamily 4a/b P450 enzymes in kidneys and livers derived from *CYP4A11* transgenic mice, suggesting that changes in the redox state of these enzymes might have relevance to the local production of 20-HETE.

RESULTS

Stimulation of P450 4A11 ω-Hydroxylation Activity by Reducing Agents—In previous work the rates of *ω*-hydroxylation of lauric acid varied considerably, from 9-21 min^{-1}, under varying conditions (4). When P450 4A11 was pretreated with either dithiothreitol (DTT) or *tris*(carboethoxy)phosphine (TCEP) reagents in our preliminary experiments (Fig. 1), *ω*-hydroxylation activity was routinely increased two- to four-fold. Similar results were found with reduced glutathione (results not presented). The ratio of the two major products, 11- and 12-hydroxy lauric acid, remained constant with this activation (results not presented). These results indicated that P450 4A11 has a thiol-dependent redox sensitivity, which was investigated further. Redox-dependent activation was also reflected in the increase in k_{cat} values for both the wild-type and F434S (*rs1126742*) (8) variants of P450 4A11 (2.1-fold) (Figs. 2*A,* 2*B*). The K_m values with and without DTT remained constant between the wild-type enzyme (63 ± 10 μM and 62 ± 15 μM, respectively) and the F434S variant (67 ± 7 μM and 58 ± 10 μM, respectively) (Figs. 2*A,* 2*B*). Collectively, these results indicate that both wild-type and F434S variant P450 4A11 are activated in a reducing environment, which may have biological relevance *in vivo*.

Ten other human P450 enzymes were tested for thiol-dependent activation with their relevant substrates (Table 1). The highest stimulation observed among these was P450 2C9, with only a 33% increase. The redox sensitivity of P450 4A11 was unique among human P450 enzymes examined here.

Oxidative Inhibition of P450 4A11—P450 4A11 hydroxylation activity was inhibited by H_2O_2. This inhibition occurred in a time-dependent manner with an 80% loss in activity occurring within 15 minutes (Fig. 3), a rate much higher than reported for uncatalyzed sulfenylation of thiols (27). Fifty percent activity loss occurred at a concentration of 140 μM H_2O_2 (Fig. 4).

Site-directed Mutagenesis—P450 4A11 encodes eight cysteinyl residues in the translated protein, and five of these cysteines were mutated to serines. Cys-457 corresponds to the proximal heme ligand and could not be changed (28), and neither C347S nor C375S produced protein with the typical P450 difference spectrum (29). Steady-state kinetic assays were done with the remaining five cysteine mutants, both with and without DTT pretreatment (Fig. 5). The response to DTT was qualitatively the same as the wild-type P450 4A11 (Fig. 2*A*), except for C200S (Fig. 5*C*) and possibly C513S (Figs. 5*A*, 5*E*), but these analyses did not implicate any of these five cysteines as being involved in the modulation of hydroxylation activity observed in the wild-type enzyme. The major conclusion was that none of these five cysteines are critical to the normal activity of P450 450 4A11, leaving only the non-mutated Cys-347, Cys-375, and Cys-457 as candidates for the oxidation-reduction phenomenon.

Identification of a Sulfenic Acid—A portion of oxidized P450 4A11 treated with each of several different concentrations of H_2O_2 was treated with d_6-dimedone (co-incubation) and subsequently counter-alkylated with (d_0-) iododimedone (30) (Fig. 6). The alkylated protein was digested with trypsin and analyzed by LC-MS/MS (Fig. 7); integrated areas of extracted ion chromatograms for the heavy (sulfenic acid-modified) and light (free thiol) were compared using the program Skyline (31). Sulfenylation of (the heme-thiolate ligand) Cys-457 coincided with the attenuation of enzymatic activity observed with increasing concentrations of H_2O_2 (Fig. 8, Supplemental Fig. S1, S2). Oxidation of the heme-thiolate ligand would lead to an inability of the heme iron to effectively activate oxygen and carry out catalysis.

This sulfenylation, however, did not exclude the possibility for thiol oxidation to occur in the form of intra- or intermolecular disulfide bonds for other P450 4A11 thiols. An isotope-coded affinity tagging (ICAT) approach was developed using d_5/d_0-iodoacetanilide (32,33) (Fig. 6). Briefly, samples were treated with varying concentrations of H_2O_2 and thiols were then trapped using a trichloroacetic acid precipitation (34). Protein was then pelleted by centrifugation, resuspended, and treated with d_5-iodoacetanilide to alkylate free thiols (35). The protein was then precipitated and resuspended in reducing buffer to reduce disulfide bonds (and any unreacted sulfenic acids) and alkylated with d_0-iodoacetanilide. Tryptic peptides were analyzed via LC-MS/MS and the area ratios of alkylated deuterated/non-deuterated thiol containing peptides were analyzed. This experiment showed no differences in ratios between a reduced P450 4A11 protein control and up to 1 mM H_2O_2 (Supplemental Data Fig. S2). Seven of the eight cysteines in P450 4A11 maintained at least 60% reduction (i.e., >60% d_0 labeling) with only Cys-513, the carboxy-terminal cysteine, being oxidized further with increasing H_2O_2.

Spectral Analysis of Heme-thiolate Oxidation—Spectral properties of P450 4A11 were used to further address the proteomic results, i.e. to address the hypothesis that the sulfenic acid moiety is disrupting the iron coordination of the heme, TCEP-treated P450 4A11 was treated with H_2O_2, reconstituted with NADPH-P450 reductase, deaerated, and placed under an anaerobic atmosphere of CO. Following the addition of NADPH, spectra were recorded for TCEP-reduced (Fig. 9*A*) and H_2O_2-oxidized (Fig. 9*B*) P450 4A11. The H_2O_2-oxidized protein showed increased absorbance at 420 nm for the CO-bound form. Sodium dithionite was added to these samples, which increased the absorbance of the oxidized enzyme at 450 nm and decreased the absorbance at 420 nm. NADPH-P450 reductase is able to reduce ferric heme to the ferrous state (allowing CO binding) but cannot reduce the sulfenic acid, leading to an inactive protein due to the loss of the thiolate axial coordination. However, dithionite is able to reduce a sulfenic acid (36), allowing for the reduced thiolate to re-ligand with the heme-iron (Fig. 10). The change in A_{450} upon the addition of dithionite in Fig. 9B corresponds to an increase of ~ 0.3 μM P450 (~ 30% total, uncorrected for loss of P450 in the degassing procedure), somewhat less than predicted from the LC-MS labeling study (Fig. 8).

Sulfenylation of Family 4 P450 Enzymes in a CYP4A11 Transgenic Mouse Model—To determine if this oxidative modification of P450 4A11 occurs *in vivo*, a *CYP4A11* transgenic mouse

model was used (20). Liver and kidney tissues from four male mice were harvested and subcellular fractionation was done immediately. Microsomes were obtained within three hours of tissue harvesting via differential centrifugation and, as with the recombinant protein, incubated with either buffer, d_6-dimedone, or d_6-dimedone supplemented with 500 μM H_2O_2 (Fig. 6). These labeled samples were then treated with catalase, reduced, counter-alkylated with (d_0-) iododimedone, and digested with chymotrypsin. Chymotrypsin was used to produce peptides containing the heme-ligand cysteine unique to both P450s 4A11 and 4a12 in kidneys of male mice (Supplemental Fig. S3) (37). The microsomal chymotryptic peptides were analyzed via LC-MS/MS and the resulting peak area ratios were quantitated. The heme-thiolate Cys-457 of P450 4A11 showed ~ 75% dimedone labeling (sulfenylation) in both the dimedone and H_2O_2-supplemented samples in the kidney microsomes of three mice and ~40% labeling in the liver microsomes (Figs. 11*A,* 11*B*, Supplemental Data Fig. S4). One mouse was considerably younger (age of 6 weeks at time of harvest, compared to the other three (two of which which were 3 months old and one was 7 months old) and the expression of P450 4A11 was greatly diminished compared to the older mice, as judged by peptide recovery. Interestingly, murine P450s 4a12 (Fig. 11*C,* 11*D*, Supplemental Data Fig. S5) and 4b1 (Fig. 11*E*, Supplemental Data Fig. S6) also showed significant sulfenylation of the respective heme-thiol ligands. The younger mouse had consistently lower levels of sulfenylation of the heme binding peptide for all of the Family 4 P450s in the kidneys and lower levels of P450 4a12 in the liver, but the sulfenylation of P450 4A11 in the liver was not different form the older mice.

DISCUSSION

We have shown that H_2O_2 reacts with the heme-thiolate cysteine of P450 4A11 to form a sulfenic acid and disrupt the iron-sulfur coordination. Five of the eight Cys residues in the protein were shown not to be essential for activity (Fig. 5), and the heme proximal ligand Cys-457 was identified as the major site of oxidation by modification and proteomic analysis (Figs. 7, 8). It is well-established that breaking this bond will also convert P450 to an inactive form, cytochrome P420 (38,39). The accessibility of the heme thiolate ligand has been established in studies with mercurials, as well as the conversion to the inactive cytochrome P420 (40,41).

The concentration of H_2O_2 required to inhibit P450 4A11 (Fig. 4) is within a physiological range (42) and was shown to be reversible via reduction by thiols (Fig. 1). P450 enzymes are known to produce H_2O_2 in conjunction with NADPH-P450 reductase and NADPH, with or without substrate present (43). H_2O_2 production was measured (43) for a typical reaction containing 0.2 μM P450 4A11, 0.4 μM NADPH-P450 reductase, the NADPH-generating system, and 100 μM lauric acid and determined to be 5 μM min^{-1}, i.e. 25 nmol H_2O_2 produced min^{-1} (nmol P450 4A11)$^{-1}$. Typical incubations with lauric acid or arachidonic acid are conducted for two to three times this long, and the concentration of H_2O_2 produced should be negligible in proportion to the amount needed to inhibit the enzyme (Fig. 4).

Thiol activation is common in *in vitro* (25). The activation seen in the case of P450 4A11 was considerably higher than with any other P450s tested (Table 1), indicating that this redox sensitivity is rather unique among the human P450s tested. Although numerous P450 purification protocols include dithiothreitol or β-mercaptoethanol (44,45), it is not clear that this is necessary in most cases.

Oxidation of P450 4A11 with H_2O_2 led to an attenuation of enzymatic activity (Figs. 3, 4). This loss of activity was correlated with an increased observation of dimedone alkylation (sulfenylation) at Cys-457, the heme-thiolate ligand (Figs. 7, 8). Sulfenic acid modifications have been directly implicated in the regulation of numerous enzymatic processes including glyceraldehyde-3-phosphate dehydrogenase, peroxiredoxin, epidermal growth factor receptor, and others (26). However, sulfenic acid formation involving disruption of heme-iron coordination is unprecedented to our knowledge. Choudhury et al. (46) mutated the cytochrome *c* peroxidase distal histidine ligand to a cysteine and observed a cysteic acid (cysteine sulfonic acid) in a crystal

structure of the cysteine mutant, with a sulfonate oxygen coordinated to the heme. They observed activity but it was markedly lower than that of the unmodified enzyme. These results were interpreted as the heme iron itself oxidizing the cysteine, as a substrate. This is an appropriate conclusion, in that peroxidases generally have non-Cys heme ligands (47,48). Nitrile hydratase enzymes are known to coordinate iron or cobalt with both sulfenylated and sulfinylated thiols; additionally, the sulfenic acid is essential for the formation of the carbamate product (49). Our results do not discern whether the sulfenylated thiol is still (weakly) coordinated to the heme or if the coordination completely disrupted in P450 4A11. Dimedone, however, can react with sulfenamides as well as sulfenic acids (50) and such reactions would provide similar results in these experiments as sulfenic acid. If a sulfenamide was indeed the cause of this redox modulation, generally thiol oxidation to sulfenic acid would occur first followed by subsequent condensation with a backbone nitrogen to form the sulfenamide (50).

ICAT analysis with iodoacetanilide did not provide evidence for a disulfide bond. α-Haloketones react with sulfenic acids to form sulfoxides (51), so these peptides would not be quantified in a direct analysis between d_0/d_5-alkylated peptides because the *m/z* would increase by 16, the mass of oxygen. Inaccuracy could also be due to further di- and tri-oxidation ($-SO_2^-$ and $-SO_3^-$, respectively) of cysteines. Cys-513 appeared to be the only thiol oxidized to a large extent in our analysis, although the exact nature is unknown. Additionally, Cys-347 and Cys-375 appear to have proximity to each other in the homology model (Fig. 12). The inability to express the mutated forms of these two cysteines indicates that they are probably important for structural and/or conformational integrity, but our ICAT analysis does not indicate that either thiol is oxidized.

Taken together the mutant analysis, dimedone labeling, and ICAT labeling methods show that cysteines other than Cys-457 are oxidized in P450 4A11 but do not appear to directly inactivate the protein or are correlated with the loss of activity. The oxidation or mutation of these ancillary cysteines could produce slight conformational changes, but these changes would not produce the spectral change at 450 nm that sulfenylation of Cys-457 does.

Detection of sulfenylation in murine kidneys and livers provides a physiological context for this modification. The high percentage of dimedone alkylation seen in the P450 4A11, 4a12, and 4b1 heme peptides was surprising in that this would imply that a large percentage of the Family 4 P450 enzymes is constitutively inactive in the kidney. One possible explanation could be that, since 20-HETE is a very potent vasoconstrictor with submicromolar activity (52,53), these enzymes are very tightly regulated and sulfenylated enzymes could act as a reserve mechanism. Conversely, if an increase in vascular tone is required quickly, Family 4 P450 enzymes could be reduced quickly and be available for production of 20-HETE. P450 4A11 sulfenylation was observed to a lesser degree in liver. This may be due to the larger reducing potential in glutathione stores the liver has compared to the kidney (54).

One unique feature of Subfamily 4A P450 enzymes is the covalent binding of the heme prosthetic group to the enzyme through a conserved glutamic acid residue (55,56). This unique feature may allow for easier re-coordination of the reduced thiol with an immobilized heme iron. In recombinant P450 4A11 it is reported that approximately 25% of the enzyme has covalently bound heme (56), but the fraction has not been determined in human samples. Rodent subfamily 4A P450 enzymes have higher percentages of heme covalently bound to the enzyme (56). LeBrun et al. (56) suggest that this covalent binding may contribute to differences in substrate binding rates and enzymatic regioselectivity.

A recent crystal structure of recombinant rabbit P450 4B1 shows complete adduction of the heme through a bond between a heme methyl group and Glu-310 (analogous to Glu-321 in P450 4A11) (57). In examining the alignment of mouse P450 4b1 and rabbit P450 4B1 (uniport.org), these two enzymes share 86% identity and 95% similarity. A modeled structure shows a relatively open conformation on the proximal side of the

protein (Fig. 12). Cysteines that were mutated in this study are located in the peripheries of the protein, away from the proposed active site, and likely do not influence enzyme function.

Disruption of the iron-sulfur coordination would alter the absorbance properties of P450 4A11 (Fig. 10). Under an anaerobic CO atmosphere, NADPH-P450 reductase can reduce ferric heme to its ferrous state, allowing CO to bind. This CO-bound state has absorbance with λ_{max} at 450 nm if the heme-thiolate ligand is intact. When this coordination is disrupted (via sulfenylation in this case), the CO-binding spectrum was shifted to a λ_{max} at 420 nm (Figs. 9 and 10). Interestingly, the addition of dithionite after reduction with NADPH-P450 oxidoreductase reduces the sulfenic acid (36) and allows for re-coordination of the thiolate-heme complex. The observation of a sulfenylated heme-thiolate ligand has probably been overlooked previously because of the common laboratory practice of determining P450 concentration using dithionite as the reducing agent for obtaining P450 difference spectra.

In summary, P450 4A11 seems to show a unique activation under reducing conditions compared to other P450 enzymes tested. Conversely, H_2O_2 inhibits the enzymatic activity of the enzyme. Sulfenic acid formation of the heme thiolate ligand was detected by labeling and LC-MS analysis (Figs. 7, 8) and was verified spectrally (Fig. 9). The physiological relevance of the modification was demonstrated with the identification of sulfenylated P450s in freshly isolated murine kidneys and livers. This modification is a potentially important observation that may have implications in other P450s, as shown by our results with the mouse P450 4a and 4b enzymes. Sulfenylation could provide for biological regulation of P450 4A11 and its production of the potent vasoconstrictor 20-HETE. As mentioned previously, 20-HETE has been shown to induce ROS formation as well as play an important role in blood pressure control, which is known to be mediated by ROS production (58). The extent of sulfenylation of 4A/a P450 enzymes in tissues may provide a mechanism to reduce the production of 20-HETE.

EXPERIMENTAL PROCEDURES

Chemicals—[1-^{14}C]-Lauric acid was obtained from American Research Chemicals (St, Louis, MO). Lauric acid, TCEP, H_2O_2 (30% w/v), paclitaxel, tolbutamide, bufuralol, nifedipine, testosterone, progesterone, coumarin, and ethoxyresorufin were obtained from Sigma Aldrich.

Chemical Synthesis

Iododimedone—Iododimedone was prepared from dimedone (4 mmol scale) by iodination with *N*-iodosuccinimide (59). Yield 48%, mp 145-146 °C; high resolution mass spectrometry (HRMS) for $C_8H_{12}O_2I$ *m/z* 266.9882 (MH^+), found 266.9881 (Δ 0.4 ppm); ^{1}H-NMR (400 MHz, $CDCl_3$) δ 1.04 (s, 6H, $(CH_3)_2$), 2.50 (d (splitting due to I), 4H, CH_2), 6.35 (s, 1H, CHI) (literature mp 155 °C (60)).

d_6-Dimedone—A modification of the basic procedure of Yeo and Carroll (30) was used. Diethyl malonate and mesityl-d_{10}-oxide were condensed in an ethanolic solution of $NaOC_2H_5$ under reflux, followed by decarboxylation with NaOH under reflux. Following neutralization, the filtrate was collected and extracted into ethyl acetate. The product was concentrated by partial removal of solvent *in vacuo* and trituration with hexanes to yield crystalline d_6-dimedone in 85% yield. mp 147-148 °C; HRMS for $C_8H_7D_6O_2$ *m/z* 147.1292 (MH^+), obs 147.1284 (Δ 5.4 ppm); ^{1}H-NMR (400 MHz, $CDCl_3$) δ 2.52 (s, 5H, -CH_2-), 3.33 (s, 2H, CO-CH_2-CO) (61) (lit mp 145-147 °C (61)).

d_0-Iodoacetanilide—Iodoacetanilide was prepared from iodoacetic acid (2.53 mmol) and aniline (2.53 mmol) by amide coupling with dicyclohexylcarbodiimide (2.53 mmol) (62). Yield 70%, ^{1}H-NMR (600 MHz, acetone-d_6) δ 9.51 (bs, 1H, NH) 7.64 (d, 2H, *o*-Ar), 7.31 (t, 2H, *m*-Ar), 7.02 (t, 1H, *p*-Ar), 3.90 (s, 2H, CH_2I), ^{13}C-NMR (150 MHz, acetone-d_6) 167.0, 140.1, 129.7, 124.6, 120.0, 0.72.

d_5-Iodoacetanilide— d_5-Iodoacetanilide was prepared from iodoacetic acid (2.53 mmol) and d_5-aniline (2.53 mmol) by amide coupling with dicyclohexylcarbodiimide (2.53 mmol) (62). Yield 89%, ^{1}H-NMR (600 MHz, acetone-d_6) δ

9.53 (bs, 1H, NH), 3.90 (s, 2H, CH_2I), ^{13}C-NMR (150 MHz, acetone-d_6) 167.0, 139.8, 129.1, 124.1, 119.6, 0.75.

Enzymes—Human P450 4A11 (wild-type and F434S, C52S, C85S, C199S, C255S, and C512S mutants) was expressed and purified as described previously (4,63). *Escherichia coli* recombinant rat NADPH-P450 reductase and human liver cytochrome b_5 (b_5) were prepared as described by Hanna et al. (64) and Guengerich (65), respectively.

Tissue Samples— All experiments using mice were conducted with approved protocols by the Institutional Animal Care and Use Committee of Vanderbilt University and in accordance with the NIH Guide for the Care and Use of Laboratory animals. 129/Sv mice carrying one copy of the human cytochrome P450 4A11 gene (*CYP4A11*) (under control of its native promoter were generated as previously described (21)) were provided normal chow diet (Purina Laboratory Rodent 5001; St. Louis, MO) with free access to water and were housed in an Association for the Assessment and Accreditation of Laboratory Animal Care (AAALAC)-accredited, temperature-controlled facility with a 12 h light–dark cycle. All studies were conducted in mice aged 6-28 weeks of age. *CYP4A11* transgenic mice were crossed with pure Sv129 wild type mice and offspring were genotyped for the presence of a single copy of the human *CYP411* gene as previously described (21). Organs were collected from male transgenic mice immediately after sacrifice and used for microsomal preparations as described below.

Site-Directed Mutagenesis—P450 4A11 was subcloned into a pBlueScript vector to preform site-directed mutagenesis. Residues from each site were converted to serine by using the QuikChange II Site-Directed Mutagenesis Kit (Agilent Technologies). The resulting plasmids were sequenced to confirm successful mutation and subcloned into a pCW expression vector.

Enzymatic Assays—Assays were done as described previously (4) with minor changes. Typical incubations included 0.2 μM P450 4A11, 0.4 μM NADPH-P450 reductase, 0.4 μM b_5, 150 μM L-α-dilauroyl-*sn*-glycero-3-phosphocholine (DLPC, Sigma Aldrich), 100 mM potassium phosphate buffer (pH 7.4), and the indicated concentration of lauric acid ([1-^{14}C]-lauric acid, usually added as an aqueous 10 mM solution of sodium laurate) in a final volume of 0.25 ml. b_5 was included because it stimulates the catalytic activity (4). Following temperature equilibration to 37 °C for 5 min, reactions were initiated by the addition of an NADPH-regenerating system consisting of 0.5 mM $NADP^+$, 10 mM glucose 6-phosphate, and 1 IU ml^{-1} yeast glucose 6-phosphate dehydrogenase (66). Reactions generally proceeded at 37 °C for 2 min and were terminated with 1.0 ml of ethyl acetate containing 0.1% CH_3CO_2H (v/v) and, following mixing with a vortex device, the mixtures were centrifuged ($10^3 \times g$ for 10 min). A 0.8 ml aliquot of the ethyl acetate layer (upper phase) was transferred to a clean tube, and the solvent was removed under an N_2 stream.

The dried extracts were dissolved in 200 μl of 1:1 mixture of H_2O:CH_3CN containing 0.1% CH_3CO_2H (v/v) and 10 μM butylated hydroxytoluene, and aliquots were analyzed on a reversed-phase (octadecylsilane, C_{18}) HPLC column (5 μm, 2.1 mm × 100 mm (Waters, Milford, MA)) coupled with a radioactivity detector (IN/US Systems β-RAM, Tampa, FL). Reaction products and substrate were eluted at a flow rate of 0.6 ml min^{-1} using an increasing linear gradient of CH_3CN (including 0.1% (v/v) HCO_2H) from 35 to 95% (v/v) over 30 min.

Assays with P450s other than P450 4A11 were performed as described previously, with the modification of either preincubation with DTT (1 mM) for 10 min or not (the DTT remained in the reactions): P450 2C8– paclitaxel as substrate (67), P450 2C9—tolbutamide as substrate (68), P450 2D6—bufuralol as substrate (69), P450 3A4—nifedipine as substrate (70), P450 19A1—testosterone as substrate (71), P450 21A2—progesterone as substrate (72), P450 2A6—coumarin as substrate (73), and P450s 1B1, 1A1, and 1A2–7-ethoxyresorufin as substrate (74).

Protein Oxidation—Purified recombinant P450 4A11 (0.4 ml of a 10 μM stock solution, stored at -80 °C in 50 mM potassium phosphate buffer (pH 7.4) containing 20% glycerol, 1 mM DTT, and 0.1 mM EDTA) was thawed on ice and

reduced for 30 minutes by the addition of 1 mM TCEP at 4 °C. A Zeba Spin Desalting Column (Thermo) pre-equilibrated with "oxidation buffer" (100 mM potassium phosphate buffer (pH 7.4) containing 0.1 mM EDTA and sparged with Ar) was used to remove reducing agents. Reduced protein was then diluted to a concentration of 500 nM using oxidation buffer. Aliquots were treated with varying amounts of H_2O_2 or TCEP. Aliquots for the activity assay (175 pmol, described above) were incubated with H_2O_2 or TCEP for 15 minutes at 37 °C. Human erythrocyte catalase (10 units, Sigma, catalog #C3556) was added and incubations proceeded at 23 °C for 5 minutes to remove H_2O_2. These samples were used to measure lauric acid ω-hydroxylation activity as described above.

Isotope-Coded Dimedone/Iododimedone (ICDID) Labeling of Recombinant P450 4A11— Additional aliquots of oxidized protein (from above, 100 pmol) were incubated with 5 mM d_6-dimedone (from a 50 mM stock suspended in 100 mM sodium hydroxyethylpiperazinepropanesulfonate (HEPPS) (pH 8.0) containing 5% NaCl (w/v)) for 2 hours at 37 °C. Trichloroacetic acid was then added to a final concentration of 10% (v/v) and the samples were incubated on ice for 15 minutes. The enzymes in the samples were pelleted by centrifugation (12,000 × *g,* 15 min, 4 °C). The supernatant was removed from each sample, and the pellet was washed with ice cold CH_3CN. The pellet was resuspended in 20 μl of 100 mM HEPPS buffer (pH 8.0) containing 2% (w/v) SDS and 1 mM TCEP, and reduction proceeded for 30 minutes at 37 °C. (d_0-) Iododimedone (100 mM stock, in acetone) was added to a final concentration of 10 mM, and incubation was done at 23 °C in the dark for 30 minutes. Samples were subjected to SDS-PAGE (10% Bis-Tris, NuPAGE, Invitrogen) separation and stained with SimplyBlue SafeStain (Invitrogen). The M_r region corresponding to P450 4A11 was excised, digested with trypsin (8 ng/μl) for 16 hours in 25 mM NH_4HCO_3 (pH 7.8) at 37 °C and subjected to LC-MS/MS analysis.

Isotope-Coded Affinity Tag (ICAT) Labeling of Recombinant P450 4A11— Additional aliquots of reduced, buffer-exchanged protein (from above, 100 pmol) were incubated with H_2O_2 or TCEP for 15 minutes. Human erythrocyte catalase (10 units) was added and incubations proceeded at 23 °C for 5 minutes to remove H_2O_2. Trichloroacetic acid was then added to a final concentration of 10% (v/v) and the samples were incubated on ice for 15 minutes. The enzymes in the samples were pelleted by centrifugation (12,000 × *g,* 15 min, 4 °C). The supernatant was removed from each sample, and the pellet was washed with ice cold CH_3CN. The pellet was resuspended in 50 μl of 100 mM HEPPS buffer (pH 8.0) containing 2% (w/v) SDS and 10 mM d_5-iodoacetanilide, and alkylation proceeded for 30 minutes at 23 °C, with shaking in the dark. Protein was precipitated again using the same method as above to remove heavy reagent. The pellet was resuspended in 20 μl of 100 mM HEPPS buffer (pH 8.0) containing 2% (w/v) SDS and 1 mM TCEP, and reduction proceeded for 30 minutes at 50 °C. d_0-Iodoacetanilide (100 mM, in acetone) was added to a final concentration of 10 mM, and incubation was done at 23 °C in the dark for 30 minutes, with shaking. Samples were subjected to SDS-PAGE (10% Bis-Tris, NuPAGE, Invitrogen) separation and stained with SimplyBlue SafeStain (Invitrogen). The M_r region corresponding to P450 4A11 was excised, digested with trypsin (8 ng/μl) for 16 hours in 25 mM NH_4HCO_3 (pH 7.8) at 37 °C and subjected to LC-MS/MS analysis.

Preparation of Microsomes—Microsomes from freshly excised tissues were prepared with slight modifications of published methods (66). For ICDID labeling studies, the buffer (0.10 M Tris-acetate (pH 7.4) containing 0.10 M KCl, 1.0 mM EDTA, and 20 μM BHT was sparged with Ar before use. Tissue samples were homogenized using a Teflon-glass Potter-Elvehjem device and centrifuged at 10^4 × *g* for 20 min. at 4 °C. Homogenates were then treated as in (66), and the final microsomal pellets were resuspended in 100 mM HEPPS buffer (pH 8.0) containing 1 mM EDTA. Aliquots of these samples were incubated with vehicle, 10 mM d_6-dimedone, or 10 mM d_6-dimedone plus 500 μM H_2O_2 for 1 hour at 37 °C. Catalase (10 units) was added to each and incubated at 25 °C for 10 minutes to remove excess H_2O_2. Aliquots were reduced with 1 mM TCEP at 37 °C for 30 minutes and 10 mM (d_0-) iododimedone was then added. The protein

concentrations of microsomes were estimated using a bicinchoninic acid (BCA) assay (Pierce). Alkylated microsomes (60 μg protein) were subjected to SDS-polyacrylamide gel electrophoresis (10% gel, *vide supra*), and the P450 region (M_r 45-60 kDa) was excised, digested with trypsin (8 ng/μl) for 16 hours in 25 mM NH_4HCO_3 (pH 8.0) at 37 °C, and subjected to LC/MS/MS analysis as described below.

LC-MS/MS Analysis—Extracted peptides were analyzed on a nanoLC Ultra system (Eksigent Technologies, Dublin, CA) interfaced with a LTQ Orbitrap XL mass spectrometer (Thermo Scientific, San Jose, CA). Approximately 5 pmol of peptides was reconstituted in 0.1% HCO_2H (v/v) and pressure-loaded (1.5 μl min^{-1}) onto a 360 μm outer diameter × 100 μm inner diameter microcapillary analytical column packed with Jupiter octadecylsilane (C18) (3 μm, 300 Å, Phenomenex) and equipped with an integrated electrospray emitter tip. Peptides were then separated with a linear gradient formed with 0.1% HCO_2H in H_2O (solvent A) and 0.1% HCO_2H in CH_3CN (solvent B) (all v/v) by increasing from 2-45% B (v/v) over a period of 0-45 minutes at a flow rate of 500 nl min^{-1}. The spray voltage was set to 2.0 kV and the heated capillary temperature to 200 °C. Higher energy collisional dissociation (HCD) MS/MS spectra were recorded in the data-dependent mode using a Top 2 method with an inclusion list containing *m/z* values corresponding to P450 4A11 tryptic peptides, which included both d_6- and d_0-dimedonylated cysteines, determined *in silico* with Skyline software (75). MS1 spectra were measured with a resolution of 70,000, an AGC target of 1e6, and a mass range from *m/z* 300 to 1,500. HCD MS/MS spectra were acquired with a resolution of 7,500, an AGC target of 1e5, and a normalized collision energy of 35. Peptide *m/z* values that triggered MS/MS scans were dynamically excluded from further MS/MS scans for 20 s, with a repeat count of 1.

Peptide Data Analysis—Raw data files were analyzed using MyriMatch software (76) against a decoy protein database consisting of a forward and reversed human Uniprot/Swissprot database (Version 20160620). Precursor ion mass tolerance was set at 10 ppm and the fragmentation tolerance was 20 ppm for the database search. Methionine oxidation (15.9949 Da, dynamic) and cysteine modifications by d_6-and d_0-dimedone (144.1057 and 138.0681 Da, respectively, static) were searched separately as modifications. The maximum Q values of peptide spectrum matches were adjusted to achieve either a peptide or a protein false discovery rate ≤5%, using IDPicker software (Version 3.1.642.0) (77). A spectral library of peptides was then created with IDPicker and loaded into Skyline Software for confident identification of precursors pertaining to cysteine-containing peptides. MS^1 precursor quantitation was performed as described previously (31). For each peptide analyzed, integral areas for M and M+1 isotopes were used for relative quantitation.

Spectroscopy—P450 4A11 was oxidized with H_2O_2 as above but the procedure was adapted slightly for spectroscopic assays. The enzyme was diluted with oxidation buffer to 1 μM prior to introduction of 1 mM TCEP or 500 μM H_2O_2. After oxidation, 30 units catalase was added and the sample was incubated at 23 °C for five minutes. To this solution, final concentrations of 1 μM NADPH-P450 reductase, 150 μM DLPC, and 0.1 unit/ml protocatechuate dioxygenase (Sigma) were added to an anaerobic cuvette, with NADPH (300 nmol, aqueous) in a side-arm of the cuvette. Samples were degassed, 20 μM 3,4-dihydroxybenzoate (Sigma, substrate for protocatechuate dioxygenase) was added to remove oxygen (78), and samples were further degassed using a manifold attached to both vacuum and purified Ar (79,80), and placed under an anaerobic CO atmosphere. The valves of the cuvettes were sealed and multiple UV-visible absorbance spectra were recorded using an OLIS/Hewlett Packard 8452 diode array spectrophotometer (On-Line Instrument Systems, Bogart, GA). Spectra were collected from 380 to 600 nm before and after the addition of NADPH/sodium dithionite.

Acknowledgements*:* We thank the Vanderbilt Proteomics Core for running some of the LC-MS/MS samples and K. Trisler for assistance in preparation of the manuscript.

REFERENCES

1. Ortiz de Montellano, P. R., ed. (2015) *Cytochrome P450: Structure, Mechanism, and Biochemistry*. 4th ed., Springer, New York
2. Guengerich, F. P. (2015) Human cytochrome P450 enzymes, in *Cytochrome P450: Structure, Mechanism, and Biochemistry* (Ortiz de Montellano, P. R., ed.), 4th Ed., Springer, New York, pp 523-785
3. Capdevila, J. H., Wang, W., and Falck, J. R. (2015) Arachidonic acid monooxygenase: Genetic and biochemical approaches to physiological/pathophysiological relevance. *Prostaglandins Other Lipid Mediators* **120**, 40-49
4. Kim, D., Cha, G. S., Nagy, L. D., Yun, C.-H., and Guengerich, F. P. (2014) Kinetic analysis of lauric acid hydroxylation by human cytochrome P450 4A11. *Biochemistry* **53**, 6161-6172
5. Lasker, J. M., Chen, W. B., Wolf, I., Bloswick, B. P., Wilson, P. D., and Powell, P. K. (2000) Formation of 20-hydroxyeicosatetraenoic acid, a vasoactive and natriuretic eicosanoid, in human kidney. Role of Cyp4F2 and Cyp4A11. *J. Biol. Chem.* **275**, 4118-4126
6. Wu, C. C., and Schwartzman, M. L. (2011) The role of 20-HETE in androgen-mediated hypertension. *Prostaglandins Other Lipid Mediators* **96**, 45-53
7. Garcia, V., and Schwartzman, M. L. (2016) Recent developments on the vascular effects of 20-hydroxyeicosatetraenoic acid. *Curr. Opin. Nephrol. Hypertens.* **26**, 74-82
8. Gainer, J. V., Bellamine, A., Dawson, E. P., Womble, K. E., Grant, S. W., Wang, Y., Cupples, L. A., Guo, C. Y., Demissie, S., O'Donnell, C. J., Brown, N. J., Waterman, M. R., and Capdevila, J. H. (2005) Functional variant of CYP4A11 20-hydroxyeicosatetraenoic acid synthase is associated with essential hypertension. *Circulation* **111**, 63-69
9. Mayer, B., Lieb, W., Gotz, A., Konig, I. R., Aherrahrou, Z., Thiemig, A., Holmer, S., Hengstenberg, C., Doering, A., Loewel, H., Hense, H. W., Schunkert, H., and Erdmann, J. (2005) Association of the T8590C polymorphism of CYP4A11 with hypertension in the MONICA Augsburg echocardiographic substudy. *Hypertension* **46**, 766-771
10. Gainer, J. V., Lipkowitz, M. S., Yu, C., Waterman, M. R., Dawson, E. P., Capdevila, J. H., and Brown, N. J. (2008) Association of a CYP4A11 variant and blood pressure in black men. *J. Am. Soc. Nephrol.* **19**, 1606-1612
11. Laffer, C. L., Gainer, J. V., Waterman, M. R., Capdevila, J. H., Laniado-Schwartzman, M., Nasjletti, A., Brown, N. J., and Elijovich, F. (2008) The T8590C polymorphism of CYP4A11 and 20-hydroxyeicosatetraenoic acid in essential hypertension. *Hypertension* **51**, 767-772
12. Zhang, R., Lu, J., Hu, C., Wang, C., Yu, W., Ma, X., Bao, Y., Xiang, K., Guan, Y., and Jia, W. (2011) A common polymorphism of CYP4A11 is associated with blood pressure in a Chinese population. *Hypertens. Res.* **34**, 645-648
13. Williams, J. S., Hopkins, P. N., Jeunemaitre, X., and Brown, N. J. (2011) CYP4A11 T8590C polymorphism, salt-sensitive hypertension, and renal blood flow. *J. Hypertens.* **29**, 1913-1918
14. Wu, C. C., Gupta, T., Garcia, V., Ding, Y., and Schwartzman, M. L. (2014) 20-HETE and blood pressure regulation: clinical implications. *Cardiol. in Rev.* **22**, 1-12
15. Bodiga, S., Gruenloh, S. K., Gao, Y., Manthati, V. L., Dubasi, N., Falck, J. R., Medhora, M., and Jacobs, E. R. (2010) 20-HETE-induced nitric oxide production in pulmonary artery endothelial

cells is mediated by NADPH oxidase, H_2O_2, and PI_3-kinase/Akt. *Am. J. Physiol. Lung Cell. Mol. Physiol.* **298**, L564-574

16. Cheng, J., Wu, C. C., Gotlinger, K. H., Zhang, F., Falck, J. R., Narsimhaswamy, D., and Schwartzman, M. L. (2010) 20-Hydroxy-5,8,11,14-eicosatetraenoic acid mediates endothelial dysfunction via $I_\kappa B$ kinase-dependent endothelial nitric-oxide synthase uncoupling. *J. Pharmacol. Exp. Therapeut.* **332**, 57-65
17. Han, Y., Zhao, H., Tang, H., Li, X., Tan, J., Zeng, Q., and Sun, C. (2013) 20-Hydroxyeicosatetraenoic acid mediates isolated heart ischemia/reperfusion injury by increasing NADPH oxidase-derived reactive oxygen species production. *Circulat. J.* **77**, 1807-1816
18. Zeng, Q., Han, Y., Bao, Y., Li, W., Li, X., Shen, X., Wang, X., Yao, F., O'Rourke, S. T., and Sun, C. (2010) 20-HETE increases NADPH oxidase-derived ROS production and stimulates the L-type Ca^{2+} channel via a PKC-dependent mechanism in cardiomyocytes. *Am. J. Physiol. Heart Circul. Physiol.* **299**, H1109-1117
19. Lakhkar, A., Dhagia, V., Joshi, S. R., Gotlinger, K., Patel, D., Sun, D., Wolin, M. S., Schwartzman, M. L., and Gupte, S. A. (2016) 20-HETE-induced mitochondrial superoxide production and inflammatory phenotype in vascular smooth muscle is prevented by glucose-6-phosphate dehydrogenase inhibition. *Am. J. Physiol. Heart Circul. Physiol.* **310**, H1107-1117
20. Savas, Ü., Machemer, D. E., Hsu, M. H., Gaynor, P., Lasker, J. M., Tukey, R. H., and Johnson, E. F. (2009) Opposing roles of peroxisome proliferator-activated receptor α and growth hormone in the regulation of CYP4A11 expression in a transgenic mouse model. *J. Biol. Chem.* **284**, 16541-16552
21. Savas, Ü., Wei, S., Hsu, M. H., Falck, J. R., Guengerich, F. P., Capdevila, J. H., and Johnson, E. F. (2016) 20-Hydroxyeicosatetraenoic acid (HETE)-dependent hypertension in human cytochrome P450 (CYP) 4A11 transgenic mice: Normalization of blood pressure by sodium restriction, hydrochlorothiazide, or blockade of the type 1 angiotensin II receptor. *J. Biol. Chem.* **291**, 16904-16919
22. Leichert, L. I., and Dick, T. P. (2015) Incidence and physiological relevance of protein thiol switches. *Biol. Chem.* **396**, 389-399
23. Paulsen, C. E., Truong, T. H., Garcia, F. J., Homann, A., Gupta, V., Leonard, S. E., and Carroll, K. S. (2011) Peroxide-dependent sulfenylation of the EGFR catalytic site enhances kinase activity. *Nat. Chem. Biol.* **8**, 57-64
24. Little, C., and O'Brien, P. J. (1969) Mechanism of peroxide-inactivation of the sulphydryl enzyme glyceraldehyde-3-phosphate dehydrogenase. *Eur. J. Biochem.* **10**, 533-538
25. Anfinsen, C. B., and Haber, E. (1961) Studies on the reduction and re-formation of protein disulfide bonds. *J. Biol. Chem.* **236**, 1361-1363
26. Devarie-Baez, N. O., Silva Lopez, E. I., and Furdui, C. M. (2016) Biological chemistry and functionality of protein sulfenic acids and related thiol modifications. *Free Radical Res.* **50**, 172-194
27. Winterbourn, C. C., and Hampton, M. B. (2008) Thiol chemistry and specificity in redox signaling. *Free Radical Biol. Med.* **45**, 549-561
28. Poulos, T. L., and Johnson, E. F. (2015) Structures of cytochrome P450 enzymes, in *Cytochrome P450: Structure, Function, and Biochemistry*, 4th Ed. (Ortiz de Montellano, P. R., ed.), Springer, New York. pp 3-32
29. Omura, T., and Sato, R. (1964) The carbon monoxide-binding pigment of liver microsomes. I. Evidence for its hemoprotein nature. *J. Biol. Chem.* **239**, 2370-2378
30. Seo, Y. H., and Carroll, K. S. (2011) Quantification of protein sulfenic acid modifications using isotope-coded dimedone and iododimedone. *Angew. Chem., Int. Ed.* **50**, 1342-1345

31. Schilling, B., Rardin, M. J., MacLean, B. X., Zawadzka, A. M., Frewen, B. E., Cusack, M. P., Sorensen, D. J., Bereman, M. S., Jing, E., Wu, C. C., Verdin, E., Kahn, C. R., Maccoss, M. J., and Gibson, B. W. (2012) Platform-independent and label-free quantitation of proteomic data using MS1 extracted ion chromatograms in Skyline: Application to protein acetylation and phosphorylation. *Mol. Cell Proteom.* **11**, 202-214
32. Kurono, S., Kurono, T., Komori, N., Niwayama, S., and Matsumoto, H. (2006) Quantitative proteome analysis using D-labeled *N*-ethylmaleimide and ^{13}C-labeled iodoacetanilide by matrix-assisted laser desorption/ionization time-of-flight mass spectrometry. *Bioorg. Med. Chem.* **14**, 8197-8209
33. Zabet-Moghaddam, M., Kawamura, T., Yatagai, E., and Niwayama, S. (2008) Electrospray ionization mass spectroscopic analysis of peptides modified with *N*-ethylmaleimide or iodoacetanilide. *Bioorg. Med. Chem. Lett* .**18**, 4891-4895
34. Lin, T. Y., and Kim, P. S. (1989) Urea dependence of thiol-disulfide equilibria in thioredoxin: confirmation of the linkage relationship and a sensitive assay for structure. *Biochemistry* **28**, 5282-5287
35. Gupta, V., and Carroll, K. S. (2014) Sulfenic acid chemistry, detection and cellular lifetime. *Biochim. Biophys. Acta* **1840**, 847-875
36. Parsonage, D., and Claiborne, A. (1995) Analysis of the kinetic and redox properties of NADH peroxidase C42S and C42A mutants lacking the cysteine-sulfenic acid redox center. *Biochemistry* **34**, 435-441
37. Muller, D. N., Schmidt, C., Barbosa-Sicard, E., Wellner, M., Gross, V., Hercule, H., Markovic, M., Honeck, H., Luft, F. C., and Schunck, W. H. (2007) Mouse Cyp4a isoforms: Enzymatic properties, gender- and strain-specific expression, and role in renal 20-hydroxyeicosatetraenoic acid formation. *Biochem. J.* **403**, 109-118
38. Omura, T., and Sato, R. (1964) The carbon monoxide-binding pigment of liver microsomes. II. Solubilization, purification, and properties. *J. Biol. Chem.* **239**, 2379-2385
39. Imai, Y., Horie, S., Yamano, T., and Iizuka, T. (1978) Molecular properties., in *Cytochrome P-450* (Sato, R., and Omura, T., eds.), Academic Press, New York, pp 37-135
40. Murakami, K., and Mason, H. S. (1967) An electron spin resonance study of microsomal Fe_x. *J. Biol. Chem.* **242**, 1102-1110
41. Franklin, M. R. (1972) The incomplete conversion of hepatic cytochrome P-450 to P-420 by mercurials. *Mol. Pharmacol.* **8**, 711-721
42. Malinouski, M., Zhou, Y., Belousov, V. V., Hatfield, D. L., and Gladyshev, V. N. (2011) Hydrogen peroxide probes directed to different cellular compartments. *PloS One* **6**, e14564
43. Kuthan, H., and Ullrich, V. (1982) Oxidase and oxygenase function of the microsomal cytochrome P450 monooxygenase system. *Eur. J. Biochem.* **126**, 583-588
44. Guengerich, F. P., Martin, M. V., Beaune, P. H., Kremers, P., Wolff, T., and Waxman, D. J. (1986) Characterization of rat and human liver microsomal cytochrome P-450 forms involved in nifedipine oxidation, a prototype for genetic polymorphism in oxidative drug metabolism. *J. Biol. Chem.* **261**, 5051-5060
45. Guengerich, F. P., Hosea, N. A., and Martin, M. V. (1998) Purification of cytochromes P450: products of bacterial recombinant expression systems. *Methods Mol. Biol.* **107**, 77-83
46. Choudhury, K., Sundaramoorthy, M., Hickman, A., Yonetani, T., Woehl, E., Dunn, M. F., and Poulos, T. L. (1994) Role of the proximal ligand in peroxidase catalysis: crystallographic, kinetic, and spectral studies of cytochrome *c* peroxidase proximal ligand mutants. *J. Biol. Chem.* **269**, 20239-20249

47. Marnett, L. J., Weller, P., and Battista, J. R. (1986) Comparison of the peroxidase activity of hemeproteins and cytochrome P-450, in *Cytochrome P-450* (Ortiz de Montellano, P. R., ed.), Plenum Press, New York, pp 29-76
48. Everse, J., Everse, K. E., and Grisham, M. B. (1991) *Peroxidases in Chemistry and Biology,* Volumes I and II, CRC Press, Boca Raton, FL
49. Martinez, S., Wu, R., Sanishvili, R., Liu, D., and Holz, R. (2014) The active site sulfenic acid ligand in nitrile hydratases can function as a nucleophile. *J. Am. Chem. Soc.* **136**, 1186-1189
50. Forman, H. J., Davies, M. J., Kramer, A. C., Miotto, G., Zaccarin, M., Zhang, H., and Ursini, F. (2017) Protein cysteine oxidation in redox signaling: Caveats on sulfenic acid detection and quantification. *Arch. Biochem. Biophys.* **617**, 26-37
51. Gupta, V., and Carroll, K. S. (2014) Sulfenic acid chemistry, detection and cellular lifetime. *Biochim. Biophys. Acta* **1840**, 847-875
52. Imig, J. D., Zou, A. P., Stec, D. E., Harder, D. R., Falck, J. R., and Roman, R. J. (1996) Formation and actions of 20-hydroxyeicosatetraenoic acid in rat renal arterioles. *Am. J. Physiol.* **270**, R217-227
53. Sun, C. W., Falck, J. R., Harder, D. R., and Roman, R. J. (1999) Role of tyrosine kinase and PKC in the vasoconstrictor response to 20-HETE in renal arterioles. *Hypertension* **33**, 414-418
54. Hazelton, G. A., and Lang, C. A. (1980) Glutathione contents of tissues in the aging mouse. *Biochem. J.* **188**, 25-30
55. Hoch, U., and Ortiz de Montellano, P. R. (2001) Covalently linked heme in cytochrome P450 4A fatty acid hydroxylases. *J. Biol. Chem.* **276**, 11339-11346
56. LeBrun, L. A., Hoch, U., and Ortiz de Montellano, P. R. (2002) Autocatalytic mechanism and consequences of covalent heme attachment in the cytochrome P450 4A family. *J. Biol. Chem.* **277**, 12755-12761
57. Hsu, M. H., Baer, B. R., Rettie, A. E., and Johnson, E. F. (2017) The crystal structure of cytochrome P450 4B1 (CYP4B1) monooxygenase complexed with octane discloses several structural adaptations for ω-hydroxylation. *J. Biol. Chem.* **292**, 5610-5621
58. Fan, F., Ge, Y., Lv, W., Elliott, M. R., Muroya, Y., Hirata, T., Booz, G. W., and Roman, R. J. (2016) Molecular mechanisms and cell signaling of 20-hydroxyeicosatetraenoic acid in vascular pathophysiology. *Front. Biosci. (Landmark Ed.)* **21**, 1427-1463
59. Sreedhar, B., Reddy, P. S., and Madhavi, M. (2007) Rapid and catalyst-free α-halogenation of ketones using *N*-halosuccinamides in DMSO. *Synth. Commun.* **37**, 4149-4156
60. Goswami, P., Ali, S., Khan, M. M., and Khan, A. T. (2007) Selective and effective oxone-catalysed α-iodination of ketones and 1, 3-dicarbonyl compounds in the solid state. *Arkivoc* **15**, 82-89
61. Shriner, R. L., and Todd, H. R. (1943) 5,5-Dimethyl-1,3-cyclohexanedione. *Org. Synth.* **Coll. Vol. 2**, 200-202
62. Niwayama, S., Kurono, S., and Matsumoto, H. (2003) Synthesis of ^{13}C-labeled iodoacetanilide and application to quantitative peptide analysis by isotope differential mass spectrometry. *Bioorg. Med. Chem. Lett.* **13**, 2913-2916
63. Kawashima, H., Naganuma, T., Kusunose, E., Kono, T., Yasumoto, R., Sugimura, K., and Kishimoto, T. (2000) Human fatty acid ω-hydroxylase, *CYP4A11*: Determination of complete genomic sequence and characterization of purified recombinant protein. *Arch. Biochem. Biophys.* **378**, 333-339
64. Hanna, I. H., Teiber, J. F., Kokones, K. L., and Hollenberg, P. F. (1998) Role of the alanine at position 363 of cytochrome P450 2B2 in influencing the NADPH- and hydroperoxide-supported activities. *Arch. Biochem. Biophys.* **350**, 324-332

65. Guengerich, F. P. (2005) Reduction of cytochrome b_5 by NADPH-cytochrome P450 reductase. *Arch. Biochem. Biophys.* **440**, 204-211
66. Guengerich, F. P. (2014) Analysis and characterization of enzymes and nucleic acids relevant to toxicology, in *Hayes' Principles and Methods of Toxicology* (Hayes, A. W., and Kruger, C. L., eds.), 6th Ed., CRC Press-Taylor & Francis Boca Raton, FL, pp 1905-1964
67. Vaclavikova, R., Soucek, P., Svobodova, L., Anzenbacher, P., Simek, P., Guengerich, F. P., and Gut, I. (2004) Different *in vitro* metabolism of paclitaxel and docetaxel in humans, rats, pigs, and minipigs. *Drug Metab. Dispos.* **32**, 666-674
68. Yamazaki, H., Gillam, E. M., Dong, M. S., Johnson, W. W., Guengerich, F. P., and Shimada, T. (1997) Reconstitution of recombinant cytochrome P450 2C10(2C9) and comparison with cytochrome P450 3A4 and other forms: Effects of cytochrome P450-P450 and cytochrome P450-b_5 interactions. *Arch. Biochem. Biophys.* **342**, 329-337
69. Hanna, I. H., Kim, M. S., and Guengerich, F. P. (2001) Heterologous expression of cytochrome P450 2D6 mutants, electron transfer, and catalysis of bufuralol hydroxylation: The role of aspartate 301 in structural integrity. *Arch. Biochem. Biophys.* **393**, 255-261
70. Yamazaki, H., Nakano, M., Imai, Y., Ueng, Y. F., Guengerich, F. P., and Shimada, T. (1996) Roles of cytochrome b_5 in the oxidation of testosterone and nifedipine by recombinant cytochrome P450 3A4 and by human liver microsomes. *Arch. Biochem. Biophys.* **325**, 174-182
71. Sohl, C. D., and Guengerich, F. P. (2010) Kinetic analysis of the three-step steroid aromatase reaction of human cytochrome P450 19A1. *J. Biol. Chem.* **285**, 17734-17743
72. Pallan, P. S., Wang, C., Lei, L., Yoshimoto, F. K., Auchus, R. J., Waterman, M. R., Guengerich, F. P., and Egli, M. (2015) Human cytochrome P450 21A2, the major steroid 21-hydroxylase: Structure of the enzyme-progesterone substrate complex and rate-limiting C-H bond cleavage. *J. Biol. Chem.* **290**, 13128-13143
73. Yun, C. H., Kim, K. H., Calcutt, M. W., and Guengerich, F. P. (2005) Kinetic analysis of oxidation of coumarins by human cytochrome P450 2A6. *J. Biol. Chem.* **280**, 12279-12291
74. Shimada, T., and Guengerich, F. P. (2006) Inhibition of human cytochrome P450 1A1-, 1A2-, and 1B1-mediated activation of procarcinogens to genotoxic metabolites by polycyclic aromatic hydrocarbons. *Chem. Res. Toxicol.* **19**, 288-294
75. M[ac]Lean, B., Tomazela, D. M., Shulman, N., Chambers, M., Finney, G. L., Frewen, B., Kern, R., Tabb, D. L., Liebler, D. C., and M[ac]Coss, M. J. (2010) Skyline: An open source document editor for creating and analyzing targeted proteomics experiments. *Bioinformatics (Oxford, U. K.)* **26**, 966-968
76. Tabb, D. L., Fernando, C. G., and Chambers, M. C. (2007) MyriMatch: highly accurate tandem mass spectral peptide identification by multivariate hypergeometric analysis. *J. Proteom. Res.* **6**, 654-661
77. Holman, J. D., Ma, Z. Q., and Tabb, D. L. (2012) Identifying proteomic LC-MS/MS data sets with Bumbershoot and IDPicker. *Curr. Protocol. Bioinform.,* **Chapter 13**, Unit 13.17
78. Patil, P. V., and Ballou, D. P. (2000) The use of protocatechuate dioxygenase for maintaining anaerobic conditions in biochemical experiments. *Anal. Biochem.* **286**, 187-192
79. Burleigh, B. D., Jr., Foust, G. P., and Williams, C. H., Jr. (1969) A method for titrating oxygen-sensitive organic redox systems with reducing agents in solution. *Anal. Biochem.* **27**, 536-544
80. Guengerich, F. P., Krauser, J. A., and Johnson, W. W. (2004) Rate-limiting steps in oxidations catalyzed by rabbit cytochrome P450 1A2. *Biochemistry* **43**, 10775-10788

FOOTNOTES

Conflict of Interest: The authors report that they have no conflicts of interest with the contents of this article. The content is solely the responsibility of the authors and does not necessarily represent the official views of the National Institute of Health.

Author Contributions: M.E.A. synthesized d_0- and d_6-iodoacetanilide and did the dimedone and iodoacetanilide labeling experiments, LC-MS assays, spectroscopic anaerobic reduction assays, and assays of catalytic activity and analyzed results. D.K. did the site-directed mutagenesis studies. F.P.G. synthesized d_6-dimedone and (d_0-) iododimedone. L.D.N., D.K., and F.P.G. did the catalytic assays with human P450s (other than P450 4A11). C.-H.Y. did the preliminary thiol activation assays. U.S., E. F. J., and A.P. developed and raised the transgenic P450 4A11 mice. M.E.A. and F.P.G. wrote most of the manuscript. F.P.G. oversaw the project. All authors contributed to the conclusions.

The abbreviations used are: b_5, cytochrome b_5; DLPC, L-α-1,2-dilauoryl-*sn*-glycero-3-phosphocholine; DTT, dithiothreitol; HCD, higher energy collisional dissociation; HEPPS, hydroxyethylpiperazinepropanesulfonate; 20-HETE, 20-hydroxyeicosatetraenoic acid; HRMS, high resolution mas spectrometry; ICAT, isotope-coded affinity tagging; ICDID, isotope-coded dimedone/iododimedone; LC-MS/MS, combined liquid chromatography–mass spectrometry; P450 (or CYP), cytochrome P450; ROS, reactive oxygen species; TCEP, *tris*(carboxyethyl)phosphine.

Grant Support—This work was supported in part by National Institute of Health grants R35 CA090426 (FPG), R01 GM118122 (FPG), R01 DK095761 (AP), R01 CA162433 (AP), R01 HD004445 (EFJ), and T32 ES007028 (MEA), the Veterans Administration (I01 BX002025-01) (AP), and National Research Foundation of Korea (Grant NRF-2016R1A2B4006978), Republic of Korea (C.-H. Y.). MEA was also supported by American Heart Association Predoctoral Fellowship #PRE33410007. AP is the recipient of a Veterans Administration Senior Research Career Scientist award. Some of the mass spectrometry work was funded in part by National Institute of Health grant P30 CA 068485 Vanderbilt-Ingram Cancer Center Support Grant.

[S]The on-line version of this article (available at http://www.jbc.org) contains Supplemental Data.

Table 1. Effects of DTT on catalytic activities of P450 4A11 and other human P450s

Human P450	Substrate	Reaction	Catalytic activity, nmol product/min/nmol P450		
			-DTT	+DTT (1 mM)	% change
4A11	Lauric acid	12-OH	9.0 ± 1.1	38 ± 1	+ 420
2C8	Paclitaxel	6-OH	1.8 ± 0.1	1.9 ± 0.1	+ 7
2C9	Tolbutamide	1′-OH	1.1 ± 0.1	1.5 ± 0.2	+ 33
2D6	Bufuralol	4′-OH	2.9 ± 0.1	3.2 ± 0.1	+ 9
3A4	Nifedipine	Desaturation	2.0 ± 0.6	1.8 ± 0.5	- 10
19A1	Testosterone	Estrone formation	10.8 ± 0.2	10.9 ± 0.9	+ 1
21A2	Progesterone	21-OH	51 ± 10	68 ± 6	+ 30
2A6	Coumarin	6-OH	[a]	[a]	- 14
1A1	Ethoxyresorufin	(resorufin)	[a]	[a]	+ 8
1A2	Ethoxyresorufin	(resorufin)	[a]	[a]	+ 26
1B1	Ethoxyresorufin	(resorufin)	[a]	[a]	- 4

Position of hydroxylation (OH) or product indicated.

[a]Assayed using fluorescence methods but absolute amounts of product not calibrated.

Fig. 1

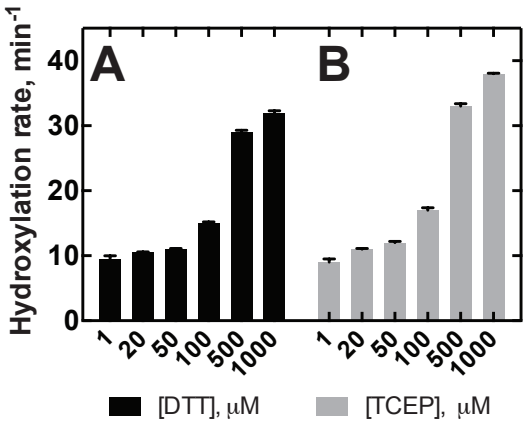

FIGURE 1. **Stimulation of lauric acid *ω*-hydroxylation activity by DTT and TCEP.** P450 4A11 was pre-incubated with varying concentrations of either (*A*) DTT or (*B*) TCEP and rates of lauric acid *ω*-hydroxylation were measured.

Fig. 2

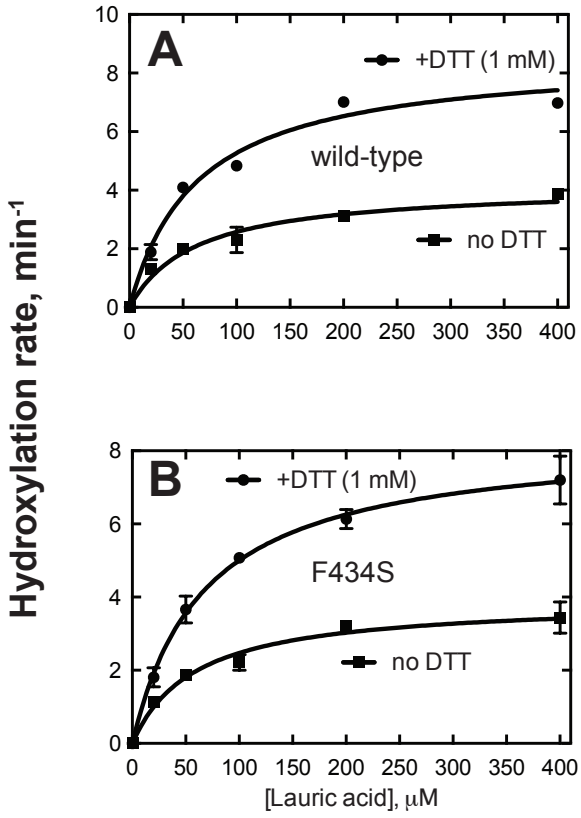

Figure 2. **Stimulation of lauric acid *ω*-hydroxylation activity by DTT**. *A*, wild-type P450 4A11 (*CYP4A11*1*); *B*, F434S variant (*rs1126742*).

Fig. 3

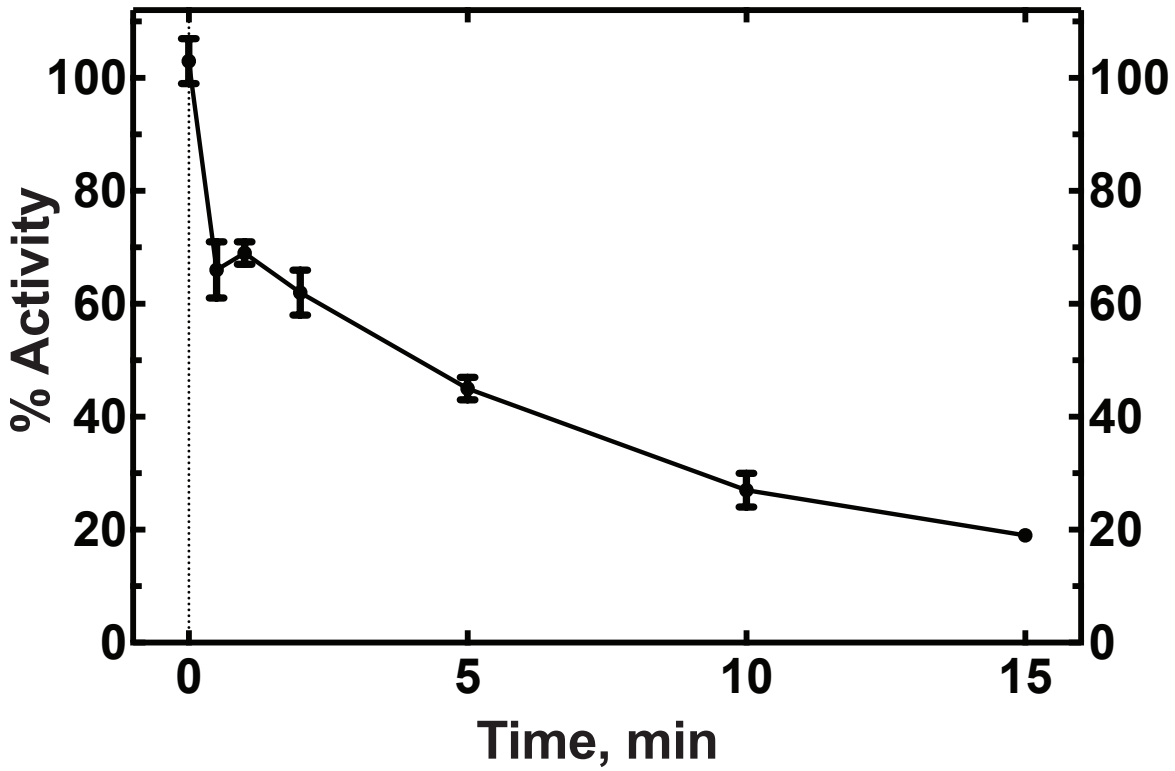

FIGURE 3. **Kinetics of loss of lauric acid ω-hydroxylation activity of P450 4A11 in the presence of H_2O_2.** P450 4A11 (500 nM) was incubated with 500 μM H_2O_2 in "oxidation buffer" (see Experimental Procedures) (pH 8.0) for the indicated times. Residual H_2O_2 was removed by treatment with human erythrocyte catalase (50 units ml^{-1}) for 10 minutes, and lauric acid ω-hydroxylation activity was measured in a reconstituted enzyme system. The initial (uninhibited) rate was 26.9 nmol ω-hydroxylation activity lauric acid formed min^{-1} (nmol P450)$^{-1}$. Results are presented as means ± SD of triplicate experiments.

Fig. 4

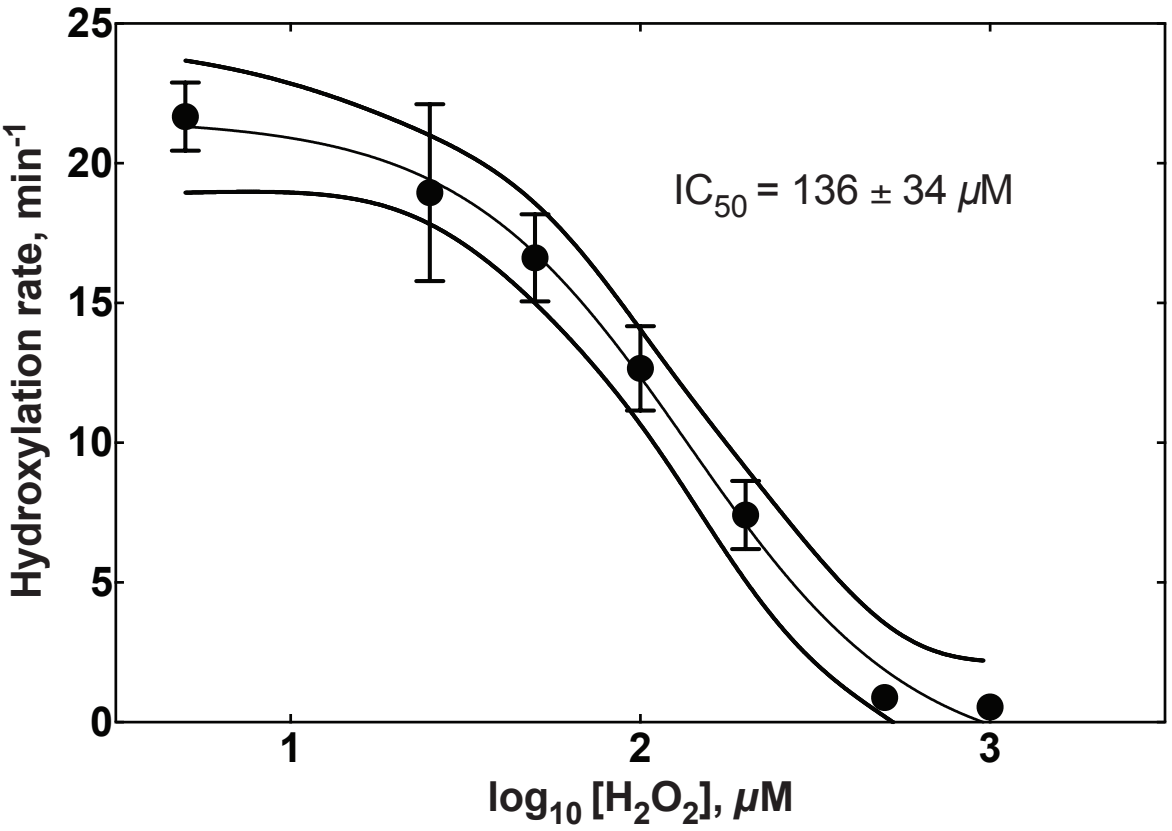

FIGURE 4. **Loss of P450 4A11 lauric acid *ω*-hydroxylation activity as a function of H_2O_2.** P450 4A11 (500 nM) was incubated with varying concentrations of H_2O_2 for 15 min at 37 °C in oxidation buffer (pH 8.0). Catalase (10 units ml^{-1}) was added to quench the residual H_2O_2 (for 10 min at 25 °C), and the remaining P450 4A11 was reconstituted and used to measure lauric acid *ω*-hydroxylation activity. Results are presented as means ± SD of triplicate experiments. The outer lines indicate 95% confidence intervals.

Fig. 5

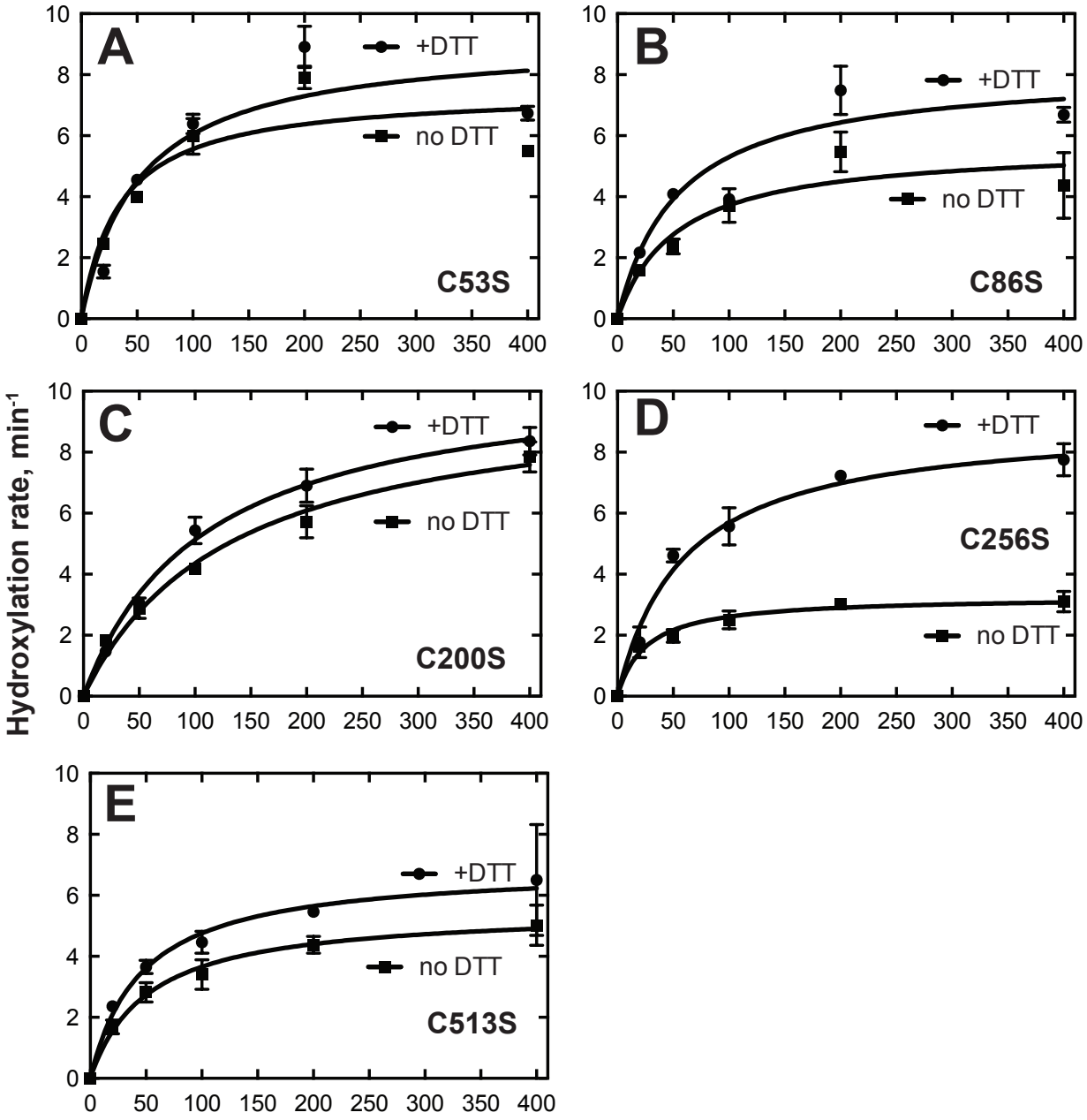

FIGURE 5. **Lauric acid ω-hydroxylation activity of Cys→Ser mutants of P450 4A11.** For experiments done at the same time with wild-type P450 4A11, see Fig. 2*A*. Assays were done in the absence (■) and presence (●) of 1 mM DTT, as indicated. *A*, C43S; *B*, C86S; *C*, C200S; *D*, C255S; *E*, C513S.

Fig. 6

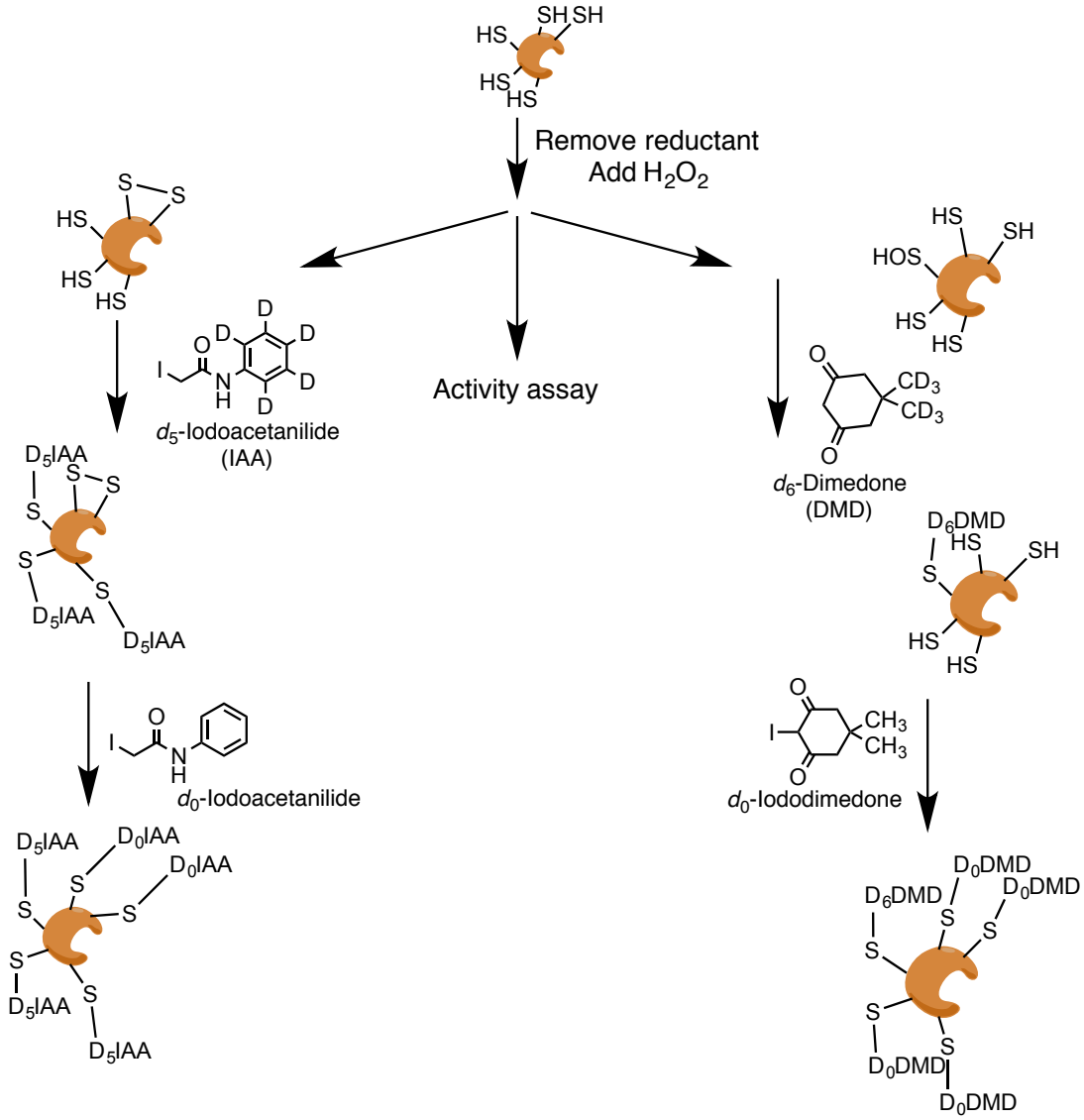

FIGURE 6. **Scheme for analysis of sulfenic acids and disulfides of P450 4A11.**

Fig. 7

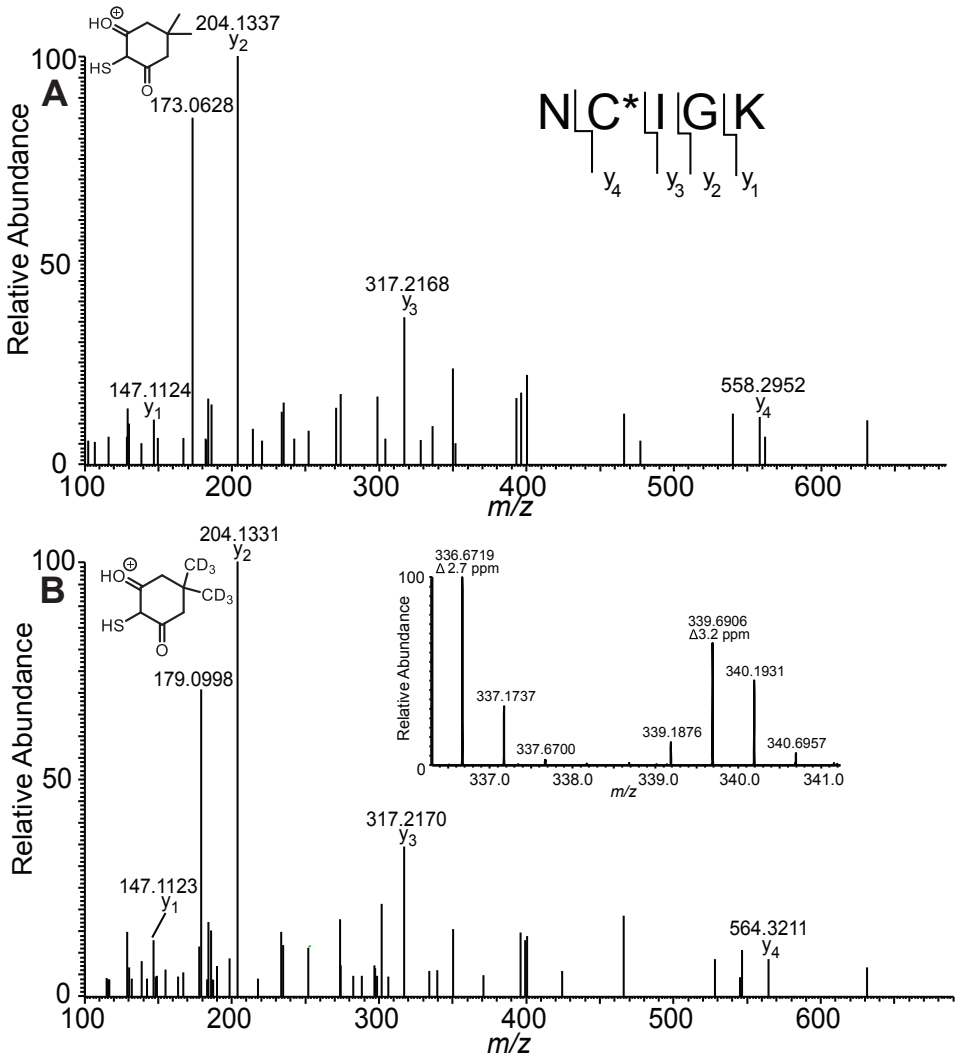

FIGURE 7. **Peptide analysis.** Annotated HCD MS/MS of the heme-thiolate containing peptide (456-NCIGK-460) alkylated with d_0-dimedone (*A*) or d_6-dimedone (*B*).

Fig. 8

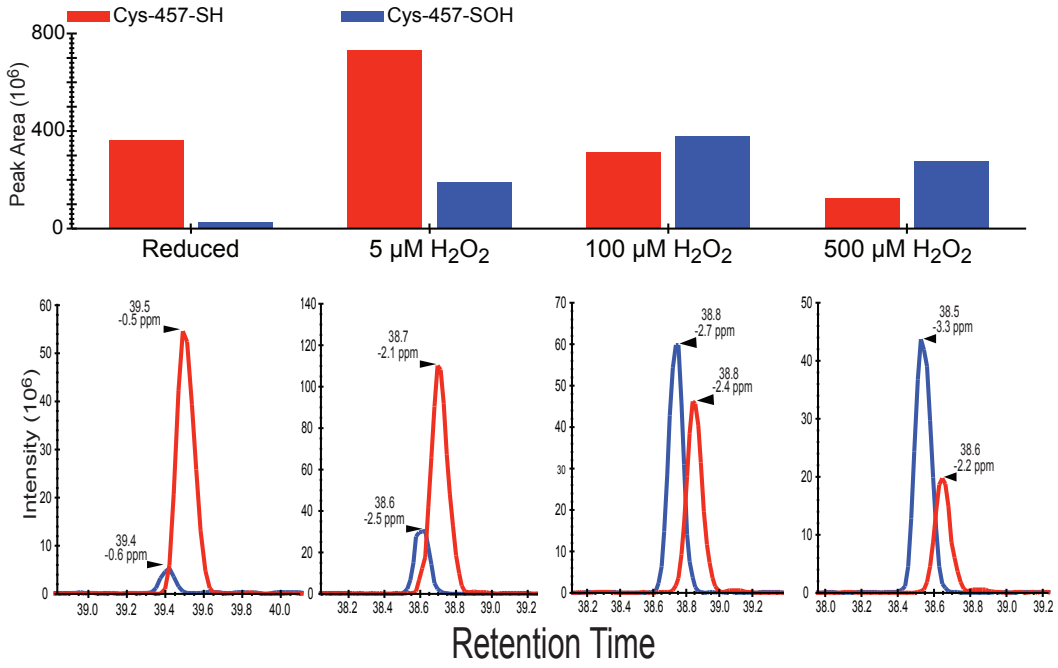

FIGURE 8. **Formation of a sulfenic acid in Cys-457 (heme thiol group) as a function of H_2O_2 concentration.** P450 4A11 samples were labeled with d_6-dimedone and and counter-alkylated with d_0-iododimedone at varying concentrations of H_2O_2. Labeled protein was then subject to trypsin digestion and LC/MS/MS analysis. Masses corresponding to Cys-457 deuterated and non-deuterated peptides were extracted and the resulting areas were integrated using Skyline software. *A*, bar graphs of comparisons of peak areas for CySH peptide (red) and CyS-OH peptide (blue); raw peaks for CySH peptide (red) and CyS-OH peptide (blue) (not normalized in each case).

Fig. 9

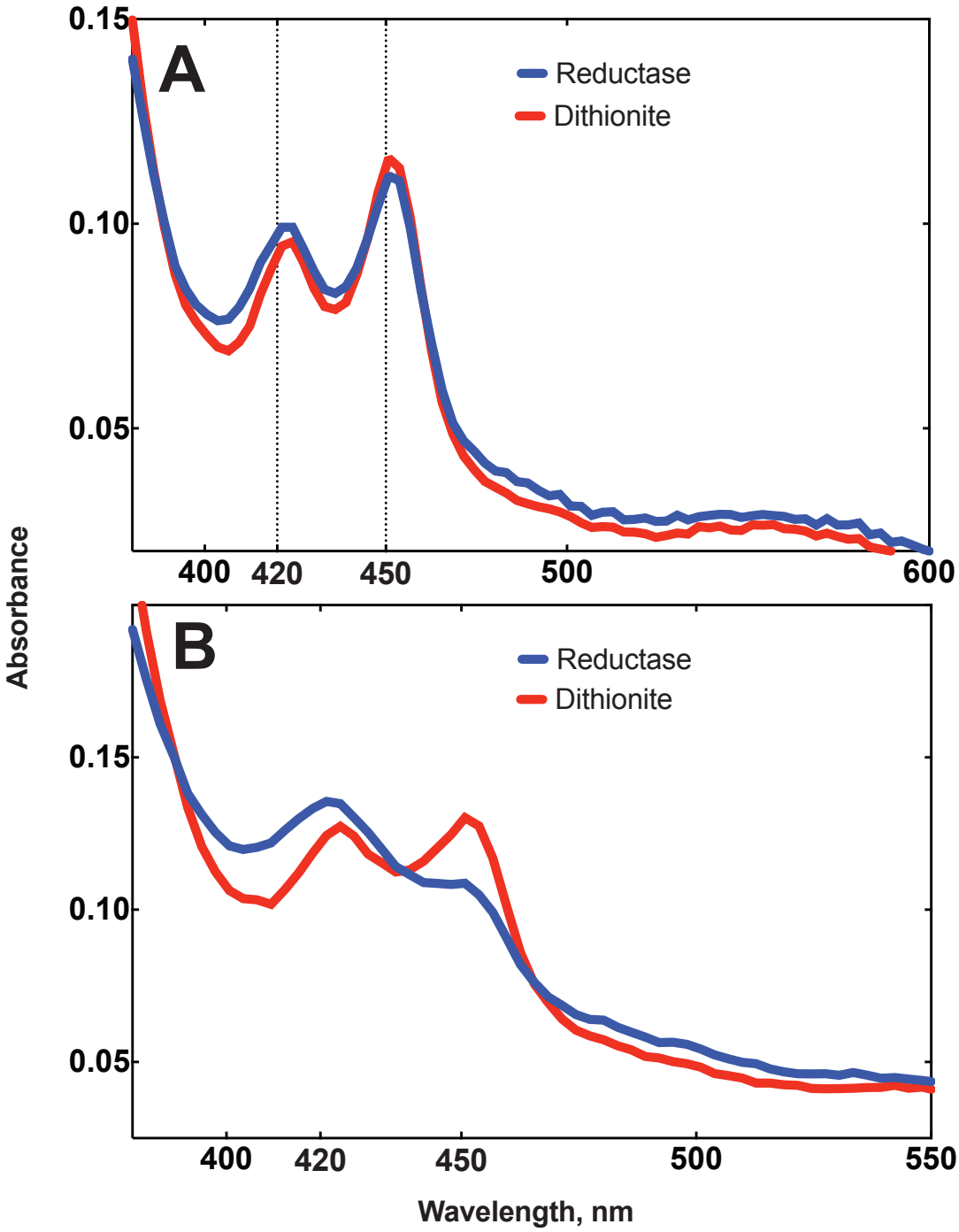

FIGURE 9. **Reduction of P450 4A11 by NADPH-P450 reductase and sodium dithionite in the presence of CO.** Reduced protein (A) and protein oxidized with 500 μM H_2O_2 (B) was deaerated and placed under an anaerobic CO atmosphere. NADPH was then added and absorbance spectra was recorded (blue). Dithionite was then added (red).

Fig. 10

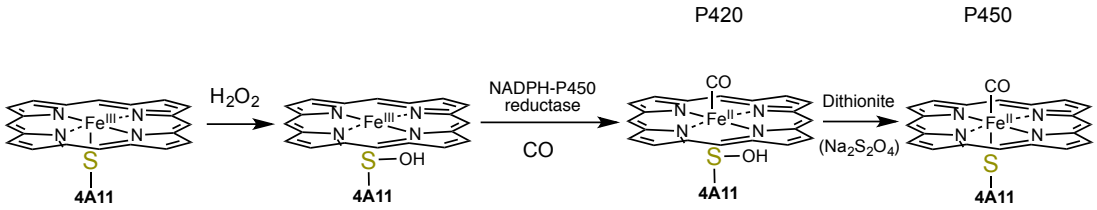

FIGURE 10. **Scheme of Cys-457 sulfenic acid formation and reduction in P450 4A11**. In the presence of H_2O_2, the heme-thiolate ligand becomes oxidized and loses its coordination with the heme iron. The sulfenic acid is not reduced by NADPH-P450 reductase but can be reduced by dithionite, reforming the heme coordination.

Fig. 11

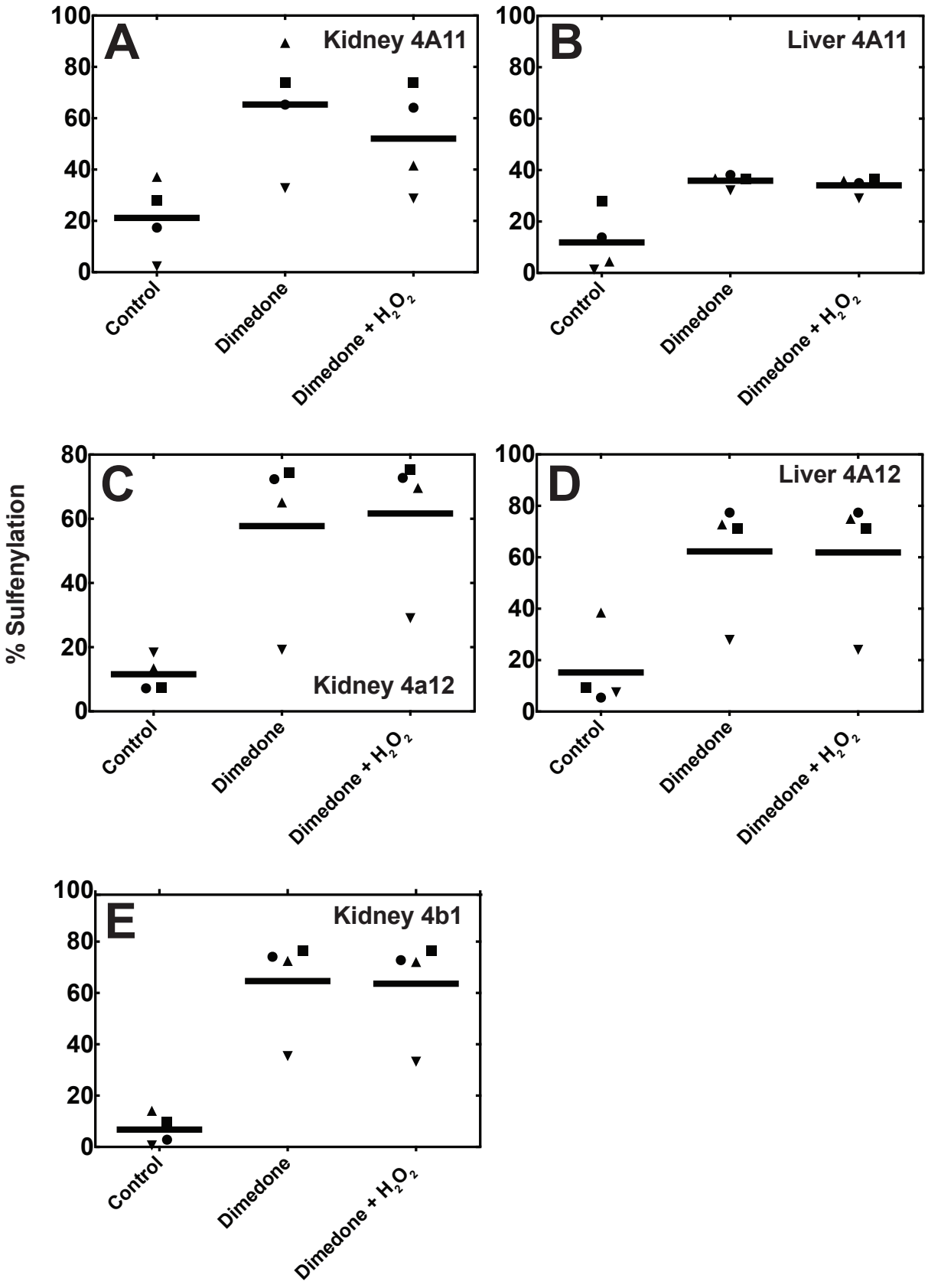

FIGURE 11. **Analysis of human and mouse P450 peptides in tg4A11 mice**. Microsomes (prepared from kidney and liver tissues of *CYP4A11* transgenic mice within 3 hours after sacrifice) were treated with either vehicle (control), d_6-dimedone, or d_6-dimedone supplemented with 500 μM H_2O_2. Integrated areas for ions corresponding to peptides of the heme-thiolate for P450s 4A11 (*A*, *B*), 4a12 (*C*, *D*), and 4b1 (*E*) were compared and reported as percent sulfenylation (percent sulfenylation = area of d_6-dimedone-labeled peptide/(area of d_6-dimedone-labeled peptide plus area of d_0-dimedone-labeled peptide)). See Experimental Procedures and Fig. 6. The p values using a Students t-test comparing control- and dimedone-treated tissue were all p <0.03 except for the P450 4a12 kidney (*C*) (p = 0.058). The mouse indicated with the label "▼" was 6 weeks old, much younger than the other three animals (two were 3 months old and one was 7 months old).

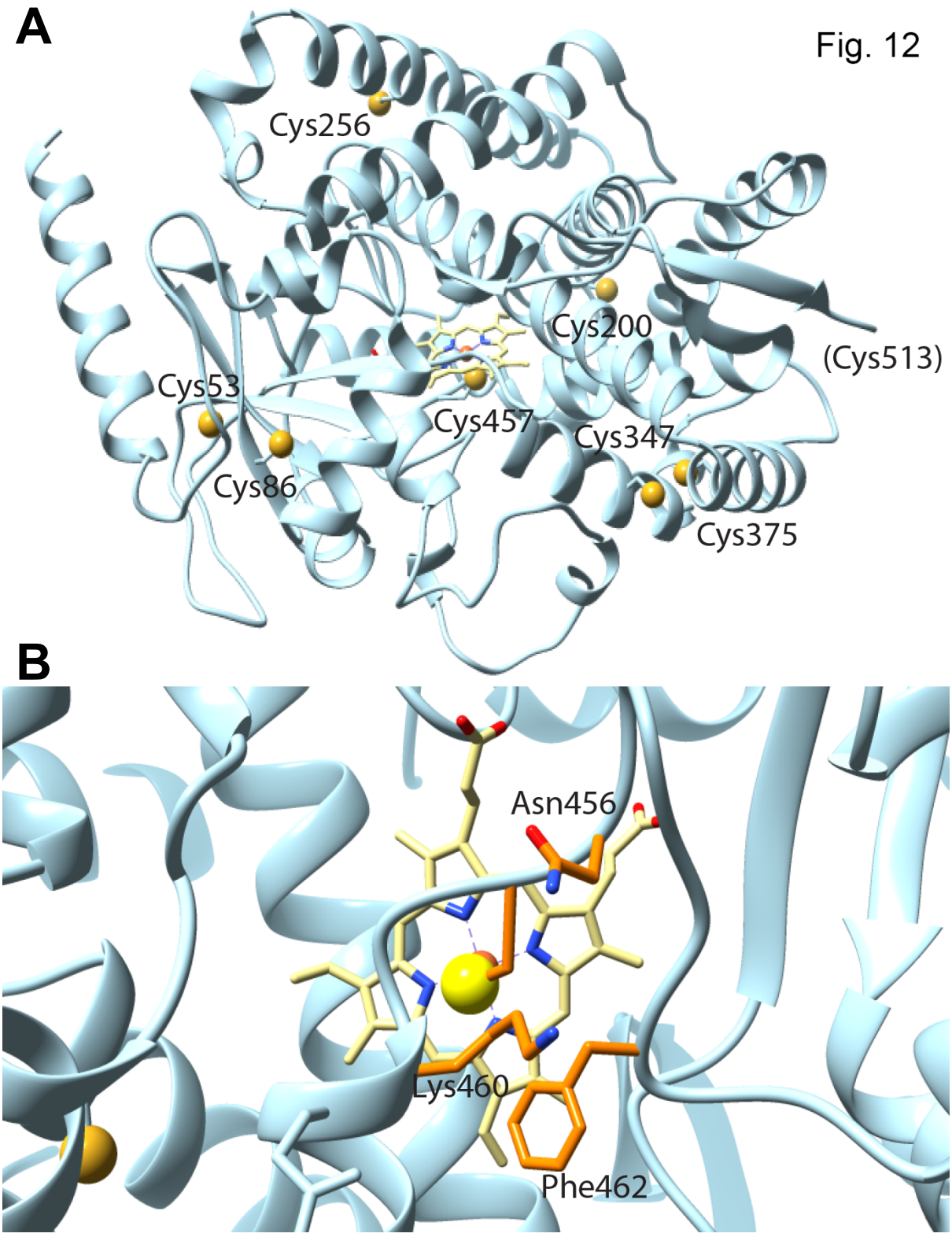

FIGURE 12. **Homology model of P450 4A11 based on crystal structure of rabbit P450 4B1** (57). *A*, All Cys residues are shown; B, positions of Asn-456, Lys-460, and Phe-462 near the heme and Cys-457 (yellow sphere).

Heme-thiolate sulfenylation of human cytochrome P450 4A11 functions as a redox switch for catalytic inhibition

Matthew E. Albertolle, Donghak Kim, Leslie D. Nagy, Chul-Ho Yun, Ambra Pozzi, Uzen Savas, Eric F. Johnson and F. Peter Guengerich

J. Biol. Chem. published online May 22, 2017
